Molar form, enamel growth, and durophagy in Cercocebus and Lophocebus

Article · July 2022

DOI: 10.1002/ajpa.24592

6 authors, including:

Debbie Guatelli-Steinberg
The Ohio State University
144 PUBLICATIONS **3,149** CITATIONS
SEE PROFILE

Mackie C O'Hara
University of Kent
28 PUBLICATIONS **174** CITATIONS
SEE PROFILE

William Scott Mcgraw
The Ohio State University
171 PUBLICATIONS **3,850** CITATIONS
SEE PROFILE

Received: 21 February 2022 | Revised: 20 June 2022 | Accepted: 29 June 2022

DOI: 10.1002/ajpa.24592

RESEARCH ARTICLE

AMERICAN JOURNAL OF BIOLOGICAL ANTHROPOLOGY
The Official Journal of the American Association of Biological Anthropologists

WILEY

Molar form, enamel growth, and durophagy in *Cercocebus* and *Lophocebus*

Debbie Guatelli-Steinberg[1] | **Gary T. Schwartz**[2] | **Mackie C. O'Hara**[1,3] | **Kaita Gurian**[1] | **Jess Rychel**[1] | **W. Scott McGraw**[1]

[1]Department of Anthropology, The Ohio State University, Columbus, Ohio, USA

[2]School of Human Evolution and Social Change and Institute of Human Origins, Arizona State University, Tempe, Arizona, USA

[3]School of Anthropology and Conservation, University of Kent, Canterbury, UK

Correspondence
Debbie Guatelli-Steinberg, Department of Anthropology, The Ohio State University, 174 West 18th Ave, Columbus OH 43210, USA.
Email: guatelli-steinbe.1@osu.edu

Funding information
National Science Foundation, Grant/Award Number: 1945008

Abstract

Objectives: To test the hypothesis that differences in crown structure, enamel growth, and crown geometry in *Cercocebus* and *Lophocebus* molars covary with differences in the feeding strategies (habitual vs. fallback durophagy, respectively) of these two genera. Relative to *Lophocebus* molars, *Cercocebus* molars are predicted to possess features associated with greater fracture resistance and to differ in enamel growth parameters related to these features.

Materials and Methods: Sample proveniences are as follows: *Cercocebus atys* molars are from the Taï Forest, Ivory Coast; *Lophocebus albigena* molars are from a site north of Makoua, Republic of Congo; and a *Lophocebus atterimus* molar is from the Lomako Forest, Democratic Republic of Congo. For μCT scans on which aspects of molar form were measured, sample sizes ranged from 5 to 35 for *Cercocebus* and 3 to 12 for *Lophocebus*. A subsample of upper molars was physically sectioned to measure enamel growth variables.

Results: Partly as a function of their larger size, *Cercocebus* molars had significantly greater absolute crown strength (ACS) than *Lophocebus* molars, supporting the hypothesis. Greater crown heights in *Cercocebus* are achieved through faster enamel extension rates. Also supporting the hypothesis, molar flare and proportional occlusal basin enamel thickness were significantly greater in *Cercocebus*. Relative enamel thickness (RET), however, was significantly greater in *Lophocebus*.

Discussion: If ACS is a better predictor of fracture resistance than RET, then *Cercocebus* molars may be more fracture resistant than those of *Lophocebus*. Greater molar flare and proportional occlusal basin thickness might also afford *Cercocebus* molars greater fracture resistance.

KEYWORDS
absolute crown strength, enamel thickness, fracture risk, hard-object feeding, teeth

1 | INTRODUCTION

The group of African monkeys referred to as mangabeys comprises species from two clades: *Cercocebus* and *Lophocebus* (Cronin & Sarich, 1976; Disotell, 1994; Groves, 1978; Harris, 2000). The two mangabey genera share several morphological and behavioral features, and it was this convergence that obscured the true phylogeny of African papionins for years (Fleagle & McGraw, 1999, 2002; Groves, 2000; Harris & Disotell, 1998; Jolly, 2001). Although similar in that they are both thickly enameled (Daegling et al., 2011; Lambert et al., 2004; McGraw et al., 2012; McGraw et al., 2014), *Lophocebus* and *Cercocebus* dentitions differ in the degree to which their premolars are molarized (Fleagle & McGraw, 1999). The premolars of *Cercocebus* are larger relative to their molars than are those of *Lophocebus*, a trait that proved informative for illuminating the diphyletic origins of these genera (Fleagle & McGraw, 1999). This difference in relative premolar size may also relate to different feeding regimes: the habitual consumption of hard foods in *Cercocebus* (Daegling et al., 2011; McGraw et al., 2012, 2014) versus the fallback consumption of hard foods in *Lophocebus* (Lambert et al., 2004).

Although the hardness of the foods these two genera consume has not been directly compared using the same methods, *Cercocebus* is believed to masticate harder foods than does *Lophocebus* (McGraw & Daegling, 2020). Moreover, these genera are known to eat hard foods in very different contexts and employ different oral processing behaviors: *Lophocebus* consumes hard foods as dietary fallbacks, when softer, preferred foods are unavailable (Lambert et al., 2004).*Cercocebus* is an habitual hard-object feeder that uses its posterior teeth to crush large, hard *Saccoglotis* seed casings not only when softer fruits are unavailable, but throughout the year (Daegling et al., 2011; McGraw et al., 2012, 2014).

Cercocebus' more frequent consumption of hard foods would expose its molars to greater opportunity for fracture, and subsequent failure, over time. In addition, although enamel is more resistant than bone to crack propagation (Bajaj et al., 2008), like bone, enamel can suffer fatigue failure under cyclic loading (Gao et al., 2016). Data do not exist that would allow us to quantify differences between *Cercocebus* and *Lophocebus* in terms of the frequency and magnitude of the loads their molars experience, but more frequent exposure to high magnitude loading would put *Cercocebus* molars at greater risk of fatigue failure. We also note that *Lophocebus*, in contrast to *Cercocebus*, uses its incisors more often during ingestion and has deeper mandibular corpora, consistent with greater incisor use (McGraw & Daegling, 2020). For all these reasons, we suggest that *Cercocebus* molars are subject to greater risk of failure over their lifetimes.

Beyond a general similarity in having thick enamel, the molars of *Lophocebus* and *Cercocebus* have yet to be systematically compared in terms of structural features (e.g., enamel thickness, the distribution of enamel across the crown, and absolute crown strength [ACS; see below]), enamel growth correlates of these structural features, and aspects of crown geometry (e.g., degree of molar flare; see below). The goal of this study is to assess whether differences between the molars of these two genera in structure, growth and crown geometry are consistent with known divergences in their feeding strategies (habitual vs. fallback durophagy) and oral processing behavior.

2 | STRUCTURAL FEATURES AND THEIR ENAMEL GROWTH CORRELATES

Despite the centrality of these two mangabey lineages to arguments about the relationship of enamel thickness to fallback and habitual durophagy (Lambert et al., 2004; McGraw et al., 2012, 2014), their enamel thickness in known from only a handful of specimens for each genus (McGraw et al., 2012). Thus, it is not yet clear if molars of these two genera are endowed with similar degrees or distributions of enamel thickness. The present study uses 2D virtual sections from 3D reconstructions of μCT renderings in the largest sample of mangabey molars evaluated yet to compare a suite of molar geometric and structural features that have been purported to relate to durophagy.

Historically, functional inferences of molar form rely heavily on the single metric of relative enamel thickness (RET), first proposed by Martin (1985). By incorporating a dental proxy for differences in body size, RET is thought to reflect dietary adaptation more accurately than do measures of absolute enamel thickness (Martin, 1985). High values of RET are presumed to reflect the ability of a crown to resist fracture when consuming hard foods and/or forestall dentine exposure caused by consumption of abrasive foods (Molnar & Gantt, 1977; Pampush et al., 2013; Rabenold & Pearson, 2011; Strait et al., 2013; Vogel et al., 2008). Thus, RET is related not only to food hardness but also to the abrasiveness of foods (Pampush et al., 2013; Rabenold & Pearson, 2011). Perhaps in part because RET relates to both food hardness and abrasiveness, Thiery et al. (2017) did not find a correlation between durophagy and RET in a sample of upper second molars drawn from 32 primate species.

Furthermore, it has recently been argued that RET is not as accurate a measure of how teeth withstand occlusal loads as a newly introduced metric, ACS, calculated as the product of tooth crown's radius and its average enamel thickness (AET; Schwartz et al., 2020). Using an engineering approach, Schwartz et al. (2020) found that ACS more closely approximates a tooth's fracture resistance than does RET, consistent with previous studies suggesting that absolute enamel thickness is directly related to crown strength (Lawn et al., 2009; Lawn & Lee, 2009; Lucas et al., 2008). Schwartz et al. (2020) suggest that RET, by contrast with ACS, is only "moderately informative" about fracture resistance and may even provide "misleading information." For example, gorillas have relatively thin enamel, but their large tooth size endows them with high ACS (Schwartz et al., 2020). It is their high ACS values, despite their low RET values, that afford gorilla molar crowns a high degree of fracture resistance consistent with the discovery of seasonal hard-object feeding in gorillas from Loango National Park, Gabon (van Casteren et al., 2019).

Given the close relationship between food material properties and tooth fracture mechanics, here we also compare *Cercocebus* and *Lophocebus* in terms of ACS. Specifically, we hypothesize that ACS, but not necessarily RET, will be greater in *Cercocebus* than in

Lophocebus, especially if *Cercocebus* molars have been selected to sustain high frequency, high magnitude loads without failing. Similarly, if *Cercocebus* molars simply afford them the ability to eat hard foods throughout the year (i.e., if they are exapted to their demanding feeding regimes), then they would also be expected have greater ACS, but not necessarily RET, than do the molars of *Lophocebus*.

Although Thiery et al. (2017) did not find a relationship between RET and durophagy, these authors did find a relationship between the distribution of enamel over molar crowns and durophagy within Cercopithecoidea. Cercopithecoids that consumed hard objects had a more uneven distribution of enamel than did nondurophagous cercopithecoids (Thiery et al., 2017). Lucas et al. (2008) predicted that more unevenly distributed enamel would be found in durophagous primates, reflecting reinforcement of enamel in regions of the crown most likely to fail during hard-object feeding.

Reinforcement of enamel at the cusp tip, in particular, has been suggested to relate to the mastication of large, hard food objects like seeds and nuts (Lucas et al., 2008). Hard objects can induce subsurface cracks at cusp tips (i.e., radial cracks; Lawn & Lee, 2009) when teeth are brought together with high force during crushing (Lucas et al., 2008). Radial cracks initiate at the enamel-dentine junction beneath the cusp, where tensile stress is concentrated during hard food mastication (Lawn & Lee, 2009). Once initiated, radial cracks can develop into "ribbon fissures" that extend downward along cusp "shoulders" and through to the enamel surface, leading to catastrophic failure (Lawn & Lee, 2009). Such cracks are more likely to extend to the enamel surface when enamel is thin, causing it to fracture (Lucas et al., 2008). On this basis, Lucas et al. (2008) predicted that durophagous species should have relatively thicker enamel at their cusp tips. Unfortunately, we determined that measures of linear cusp tip thickness had low repeatability in our study (10%–12% error on average), and therefore do not include these measurements here. We do, however, include linear measures of occlusal basin thickness, which were more reliable. Given their intimate and reciprocal relationship—because cusps crush food in opposing occlusal basins—durophagy has been suggested to be associated with particularly thick occlusal basins, as appears to be the case in orangutans (Kono, 2004). O'Hara (2021) found that several measures of occlusal basin thickness scaled to AET (Martin, 1985) were associated with durophagy in extant catarrhines, including *Cercocebus atys*.

We also examined enamel thickness along the lateral wall of functional cusps, under the assumption that thicker lateral wall enamel offers greater resistance to margin fracture. Margin cracks can result from biting on either hard or soft foods and are initiated at the enamel-dentine junction of the crown base (cervical margin) as coronal dentine expands under vertical compression (Lawn & Lee, 2009). As the crown base bulges, it is subject to tensile "hoop" stresses that promote crack extension upward along the enamel walls. Like radial cracks, margin cracks can develop into ribbon fissures, leading to catastrophic failure. Again, we expected the habitually durophagous *Cercocebus* to have proportionally greater functional side lateral wall thickness than does *Lophocebus*.

We further hypothesized that potential differences between *Cercocebus* and *Lophocebus* in AET or crown size, both of which contribute to ACS, would be linked to differences in enamel growth. We therefore investigated potential differences in enamel growth variables such as daily secretion rates (DSRs), enamel extension rates (EERs), and overall enamel formation times. Thicker enamel can be produced by faster DSRs, longer crown formation times, or both (Grine & Martin, 1988). Larger crowns—specifically those with greater crown heights—can result from increases in EERs, crown formation time, or both (Guatelli-Steinberg et al., 2012).

3 | ASPECTS OF CROWN GEOMETRY

With respect to aspects of crown geometry, we evaluated the association of cuspal geometry with habitual hard-object consumption by quantifying cusp tip angles and degree of cusp flare. Blunt, low cusps (i.e., those with more obtuse cusp tip angles) are suggested to be less subject to breakage than tall sharp cusps when eating hard foods (Kay, 1978). We also note that blunt cusps are also expected to function more efficiently than tall, sharp cusps when cracking hard objects and reducing them through grinding (Constantino et al., 2009; Jolly, 1970; Kay, 1978, 1981; Luke & Lucas, 1983).

Cusp flare (Figure 1) refers to the angulation of the cusp from cervix to cusp tip (Shimizu, 2002; Singleton, 2003; Macho & Shimizu, 2009). In terms of function, Singleton (2003) found an association between molar flare and hard-object feeding in contemporary hominoids. More specifically, it has been suggested that molar flare might buttress crowns against laterally directed forces during chewing (Macho & Shimizu, 2009). However, Macho and Shimizu (2009) suggested that lateral flare is not necessarily expected in a dedicated hard-object feeder: omnivorous macaques, for instance, exhibit lateral flare. They also cited Woda et al. (2006) who found that in humans it is primarily jaw muscle activity, not jaw kinematics, that is related to food hardness. More recent experimental studies in humans, however, suggest that while muscular activity increases as a function of food hardness, so too does lateral jaw movement (Almotairy et al., 2021; Kitashima et al., 2015; Komino & Shiga, 2017). Thus, cusp flare may serve as a buttress against laterally-directed forces during the crushing or grinding of hard foods. Here we examined "functional" cusp flare, where functional cusps are those that are involved in Phase II of the chewing cycle (Kono, 2004; Schwartz, 2000). *Cercocebus* molars are expected to exhibit greater functional cusp flare, and thus stronger buttressing, than those of *Lophocebus*. Table 1 summarizes the predictions tested in this study.

4 | MATERIALS AND METHODS

4.1 | Sample provenience and preparation

The *C. atys* sample used in this study derives from the Taï Forest of the Ivory Coast, collected by W.S.M. and members of the Taï Forest

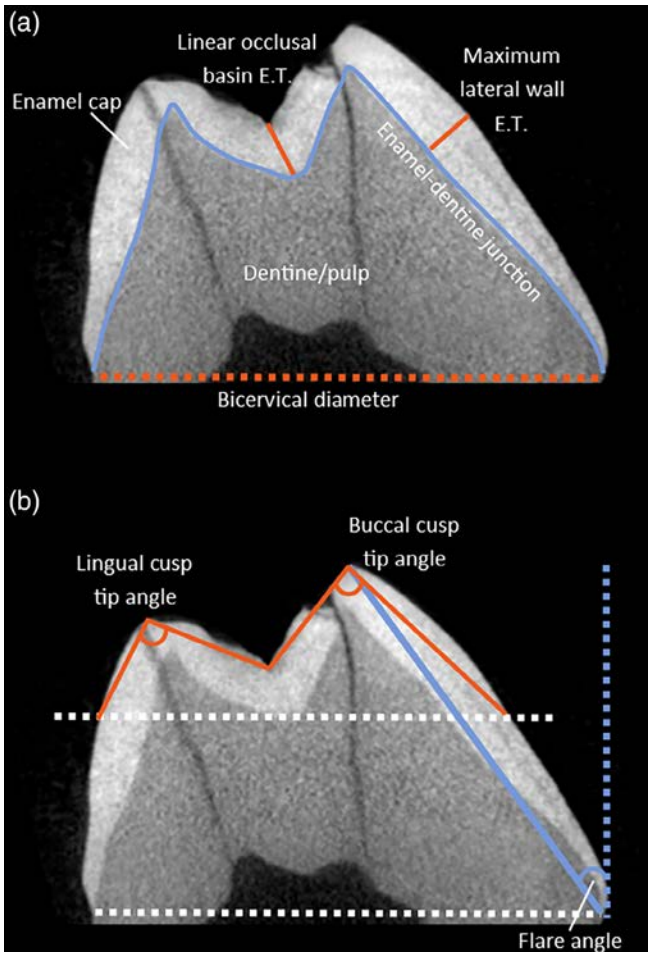

FIGURE 1 A virtual slice through the mesial cusps of a *Cercocebus* upper left third molar taken at a resolution of 22 μm (specimen TF 2010–2). (a) Reference lines for enamel thickness measurements including bicervical diameter, enamel-dentine junction, occlusal basin enamel thickness, and maximum lateral wall enamel thickness. The area of the enamel cap is visible in white, bounded by the EDJ. The dentine-pulp crown area is the area bounded by the EDJ and the bicervical diameter. (b) As a reference for cusp tip measurements, a line was drawn parallel to the bicervical diameter and tangent to the EDJ at the lowest point of the occlusal basin (dotted white lines). Lingual and buccal cusp tips angles were measured between the point where this line intersected the OES to the cusp tip (vertex of the angle) to the lowest point of the occlusal basin. The solid blue line extending from the CEJ to the cusp tip served as a reference line for measuring molar flare. Molar flare was measured as the angle between the solid blue line and a line perpendicular to the BCD (dotted blue line)

TABLE 1 Summary of predictions

Feature	Prediction	Justification
Relative enamel thickness (RET)	*Cercocebus* ≈ *Lophocebus*	*Cercocebus* and *Lophocebus* not necessarily expected to differ in RET, since RET is an indirect measure of a crown's overall fracture/abrasion resistance.
Absolute crown strength (ACS)	*Cercocebus* > *Lophocebus*	Masticatory demands of habitual durophagy are greater in *Cercocebus*.
Occlusal basin thickness (OBT)	*Cercocebus* > *Lophocebus*	*Cercocebus*' frequent consumption of hard foods may expose its molars to greater risk of through-thickness fracture of the occlusal basin.
Lateral wall enamel thickness (LWET) of functional cusps	*Cercocebus* > *Lophocebus*	*Cercocebus*' frequent consumption of hard foods may expose its molars to greater risk of margin cracking that can lead to ribbon fractures extending to the enamel surface.
Enamel growth variables	Cercocebus ≠ Lophocebus	Enamel growth variables will differ, given the diphyletic origins and different feeding regimes of these two genera.
Cusp tip angle	*Cercocebus* > *Lophocebus*	Blunt cusps are less likely to break than tall, sharp cusps when hard foods are consumed.
Flare of functional cusps	*Cercocebus* > *Lophocebus*	Greater flare would serve as a stronger buttress against laterally directed forces during crushing and grinding hard foods.

Monkey Project over the course of three decades. They are housed in the Primate Lab in the Department of Anthropology at The Ohio State University. At Taï, *C. atys* diets consist mostly of hard-foods, especially *Sacoglottis gabonensis*, which has seed casings with twice the hardness of cherry pits (Daegling et al., 2011). *C. atys* processes *S. gabonensis* seeds year-round, by placing them immediately posterior to their canines and crushing them on their premolars and molars with a powerful isometric bite (Daegling et al., 2011; McGraw et al., 2011, 2014).

The *L. albigena* sample was collected by Professor Randall Susman (Stony Brook University) near the Mambili River approximately 50 km north of Makoua in the Republic of Congo (Susman, pers. comm). Feeding data on these individuals were not collected; however, feeding data on *Lophocebus albigena* are available from Lope (Ham, 1994; Tutin et al., 1997) and Makande (Brugiere et al., 2002) Gabon, the

nearby Dja Reserve in southcentral Cameroon (Poulsen et al., 2001; Poulsen et al., 2002), and Uganda's Kibale Forest (Lambert et al., 2004; Olupot et al., 1997; Waser, 1984). At each of these sites, *L. albigena* prefers fruit but switches to seed-eating when fruit is scarce. For example, during the dry season, *L. albigena* at Lope rely on seeds of *Pentoclethera macrophylla* (Ham, 1994), which are protected by hard and tough pods (McGraw et al., 2016). Based on our reading of the literature, there is no indication that *L. albigena* is consuming hard-object foods year round, but rather is doing so seasonally. Because we are interested in generic differences (i.e., differences between *Cercocebus* and *Lophocebus*) and because our *L. albigena* sample is relatively small compared to our *C. atys* sample, we also include one *L. atterimus* specimen from Democratic Republic of Congo's Lomako Forest (McGraw, 1994).

Table 2 gives the specimen numbers and tooth types used in the current study. Not all specimens were used in every analysis; sample sizes for various measurements and statistical comparisons are provided in the Results section. Choice of right or left antimere was based on which crown appeared least worn. Sex was known for only a portion of the sample. To maintain adequate sample sizes, sex was not included as a covariate in our analyses, and as a result, remains an unknown source of potential variation. All teeth were manually extracted from maxillae and mandibles and sterilized with UV light.

4.2 | μCT methods

Extracted teeth were scanned using a Bruker Skyscan 1172 High Resolution Ex Vivo 3D X-Ray Tomography Scanner located in the Do-Gyoon Kim Laboratory at the OSU College of Dentistry. The first ten teeth were scanned at a resolution of 13 μm, but since the boundary between enamel and dentine was clearly differentiable at 22 μm, the

TABLE 2 Full dental sample

Species	Individual	Sex	Tooth types
C. atys	TF 16–5		UM1, UM2, LM1, LM2
	TF 16–9	M	UM3
	TF 16–11	F	UM3
	TF 22–26	M	UM2, UM3, LM2, LM3
	TF 22–29	M	UM2, UM3, LM3
	TF 22–46		UM1, UM2
	TF 23–10		UM2, UM3
	TF 24–3	F	UM2, LM1
	TF 94–7	F	UM2
	TF 94–9	M	UM2, UM3, LM3
	TF 94–25		UM1, UM2
	TF 2001		UM1, UM2
	TF 2008	F	UM3
	TF 2010–1		UM1
	TF 2010–2		UM2, UM3
	TF 2016	F	UM2, UM3
	TF 2019		UM1, UM2
	TF 2020		UM1, LM1
	TF 2040		LM1
	TF 2041		UM1
	TF 2106	M	UM3, LM3
	TF 2108		UM2,UM3, LM3
	TF 2138	F	UM3
	TF 22–46		UM1, UM2
	TP-91		UM2
L. albigena	85–1	F	UM1, UM2, UM3, LM1, LM2, LM3
	85–7	M	UM1, UM2, UM3, LM1, LM2, LM3
	85–17	M	UM1, UM2, UM3, LM1, LM2
	642	M	UM1, UM2, UM3, LM1, LM2, LM3
L. aterrimus	81–7	F	UM2

latter resolution was used for the remainder of the sample. RAW output files were processed with N.Recon v1.7.4.2 and then saved as TIFFs. Two-dimensional bucco-lingual planes of section (mesial and distal) were generated from 3D digital renderings of the teeth (following Skinner et al., 2015) using Dragonfly v.2021.1.0.977, passing through buccal and lingual dentine horns and perpendicular to the cervical margin. Each virtual section was then saved as a TIFF and imported into Adobe Photoshop where crown outlines were reconstructed (when necessary) prior to performing measurements.

Measurement reference lines and points are shown in Figure 1. AET was calculated as the enamel cap area divided by the EDJ length (Martin, 1985), while RET was calculated as AET divided by the square root of the dentine-pulp area bordered by the EDJ and bicervical diameter (BCD) and multiplied by 100 (Martin, 1985). ACS was calculated as the square root of the product of the coronal dentine radius (half of the BCD) and AET (Schwartz et al., 2020). Linear enamel thickness of the occlusal basin was measured as the distance between the lowest point of the occlusal basin at the EDJ and the lowest point of the occlusal basin at the outer enamel surface, or OES (Kono-Takeuchi et al., 1998; Macho & Berner, 1994; Macho & Thackeray, 1992, 1993; Olejniczak & Grine, 2006; Schwartz, 1997, 2000). Maximum lateral wall enamel thickness was measured at the widest point between the EDJ and OES, along a line perpendicular to the EDJ (Kono et al., 2002; Schwartz et al., 2020; Spoor et al., 1993; Suwa & Kono, 2005; Ulhaas et al., 1999). Proportional linear occlusal basin and lateral enamel wall thicknesses were obtained by dividing each linear measure by AET (O'Hara, 2021). Thus, "proportional thickness" scales the linear thickness of enamel in each of these regions (occlusal basin and lateral enamel wall) to the average thickness of enamel for a crown. Measures greater than 1 represent relatively thicker enamel in these regions.

To measure cusp tip angles, a line parallel to the BCD and tangent to the lowest point on the EDJ of the occlusal basin was drawn (Figure 1). Cusp tip angles were measured as the included angle between where that line intersected the OES and the angle's vertex (Figure 1). To perform measurements of cusp flare, 2D slices were rotated in ImageJ so that their BCDs were horizontal; then, a line perpendicular to the BCD was drawn. Lastly, a line connecting the CEJ to the apex of the cusp (or reconstructed cusp) on the OES was drawn (Shimizu, 2002). The angle between this line and the line perpendicular to the BCD was the angle measured for flare (Figure 1).

While there were some unworn crowns in the sample, most exhibited varying degrees of wear. Worn crowns were reconstructed following the recommendations of O'Hara and Guatelli-Steinberg (2021). These authors found that for AET and crown height measurements, crowns with limited wear (for which wear did not reach the dentine horns and/or the deepest point of the occlusal basin) accurate values were achievable with the Profile (Grine & Martin, 1988; Smith et al., 2011; Smith et al., 2012), Polynomial (Modesto-Mata et al., 2017), and Pen Tool methods (Guatelli-Steinberg et al., 2009; O'Hara et al., 2019; Saunders et al., 2007). O'Hara and Guatelli-Steinberg (2021) also found that, for crowns on which wear exposed the tips of dentine horns (what they termed "extensive wear"), it was still possible to obtain accurate AET values using the Profile or Polynomial methods. The O'Hara and Guatelli-Steinberg (2021) recommendations were followed here for AET, RET, and measurements of molar flare using the Profile method on teeth with extensive wear and incorporating the Pen Tool method if a reference tooth was not available, but wear was limited. Maximum functional lateral wall linear measurements were possible with slight wear on cusps since the dentine horn was used as a reference point. No measurements of cusp tip angles or linear occlusal basin thickness were performed on crowns with any occlusal basin wear and/or on any reconstructed crowns.

All measurements on μCT slices were made by either Kaita Gurian or Jess Rychel, whose inter-observer error was assessed. Forty-six mesial slices were measured by both Kaita Gurian and Jess Rychel for crown area, bicervical diameter, EDJ length, and maximum functional cusp linear thickness. For all these measures, average interobserver error ranged from 0.5% to 4.6%. Linear occlusal basin thickness measurements on 23 slices averaged 7.4% error, while errors for functional cusp tip angle on 24 slices and nonfunctional cusp tip angle on 23 slices averaged 2.8% and 2.9%, respectively. The higher error of the occlusal basin thickness measurements, we believe, reflects small variations in how the measurement line is angled from the lowest point of the occlusal basin to the EDJ. Flare was measured by Kaita Gurian only, whose average intra-observer error for 15 teeth was 0.8%. For calculated values (ACS, AET, and RET) average interobserver error was less than 5%.

4.3 | Histological methods

After μCT scans were made, a subset of *Cercocebus* and *Lophocebus* upper second and third molars were physically sectioned across mesial cusps following steps outlined in Reid et al. (1998), with some modifications. Using the μCT slices, we marked the plane of section on the tooth and then embedded it in epoxy resin (Buehler™ Epoxicure). We used a Buehler IsoMet low-speed saw equipped with a 5-in. diameter diamond-wafering blade. Teeth were mounted on the saw using an irregular sample chuck in order to line up the desired section plane with the blade. Despite efforts to directly cut along the desired plane, we found that we usually were able to obtain cuts directly through only one of the dentine horns of the two mesial cusps. The side of the cut block with the sharpest dentine horn was mounted on a slide with Gorilla™ epoxy and a second cut was made parallel to the first. The specimen was then ground using a target holder on a series of Buehler CarbiMet abrasive papers with successively finer grit until a thickness of approximately 100 μm was reached and microstructures (e.g., cross striations) were visible. The sample was then polished using Buehler alumina micropolish, after which the slide was dehydrated in an ethanol series and rinsed in the clearing agent Histoclear. The slide was then cover-slipped using immersion oil and imaged with a Motic BA 310 Microscope fitted with a Moticam camera. Montages at 4× were made for measurements of EDJ lengths used in calculating enamel extension rates. All enamel growth measurements were made in ImageJ by one of us (Debbie Guatelli-Steinberg).

To measure daily secretion rates (DSRs), total EDJ lengths along the crown walls were measured and divided into thirds. In each third of the crown, viewed at 40x, measurements along enamel prisms were taken across six cross-striations (5 days) within 200 μm of the EDJ. Three such measurements were taken in each third of the crown and averaged to obtain a DSR value for each region. Three measurements were taken and averaged in the occlusal basin as well, as an indicator of whether there were differences between genera in the rate of enamel secretion in this region of the crown. This set of measurements was performed because, as will be seen below, the two genera differed in the proportional thickness of their occlusal basins.

Enamel extension rates were measured in the following methods described by Dean (2009, 2012) and Guatelli-Steinberg et al. (2012). Just lateral to the tip of the dentine horn, a point along the EDJ was identified. A 200-μm line was drawn from this point outward, along an enamel prism. Where that line stopped, another line parallel to or coincident with a stria of Retzius was followed back to the EDJ (Figure 2). The point where that line intersected the EDJ was marked, and the distance along the EDJ was measured between this point and the first point (i.e., the point near the dentine horn tip). Because striae of Retzius mark the enamel-forming front at a point in time, this segment of the EDJ represents the distance over which ameloblasts differentiated during the same length of time it took for the 200 μm prism segment to form. That length of time varied depending on each third of the crown. For example, in the cuspal third of the crown, DSRs were faster than they were in the cervical third, such that the length of time it took to form the 200 μm prism length was shorter in the cuspal region than in the cervical region. The amount of time it took to form the first EDJ segment is 200 μm divided by the cuspal DSR. For example, if the cuspal DSR were 4 μm/day, then the time it took to form this first EDJ segment was 50 days. To obtain the rate of enamel extension corresponding to this segment, the EDJ segment length would then be divided by 50 days.

This "zigzag" procedure was followed down the full length of the EDJ along the crown walls (see Figure 2), with the appropriate DSR used in the enamel extension rate calculation based on crown location. In three of 26 cusps, there was a small portion (of approximately 200 μm or less of the EDJ missing at the dentine horn tip) owing to wear. In these three cases, the dentine horn was reconstructed (profile method) and a 200 μm line parallel with the first prism was drawn from the first point of the reconstructed EDJ toward the outer enamel surface. A stria of Retzius was followed from the EDJ back to the end of that line, establishing the boundaries of the first measurement.

To obtain total enamel formation time, the time it took to form each segment length was summed along the length of the entire EDJ. However, it is not possible to draw a 200 μm line along a prism near the cervix as enamel thins extensively in this region. To estimate the length of time it took to form the remainder of the crown (see Figure 2), the enamel extension rate of the preceding segment was applied to the remaining length, and then added to the summed enamel formation times of the preceding EDJ segments.

Measurement error was assessed on four molar crowns (two *Lophocebus*; two *Cercocebus*). For DSRs, there were 12 areas on these crowns where DSR had previously been measured three times and then averaged. For the 12 areas, the average DSRs from the first and second round of measurements differed by 2.1%. For EERs, 30 segments were remeasured and the new DSRs from the second round were applied to them. On average, EERS differed between the first and second round by 3.5%. The four total enamel formation times for these teeth differed between the first and second round by 1.3%.

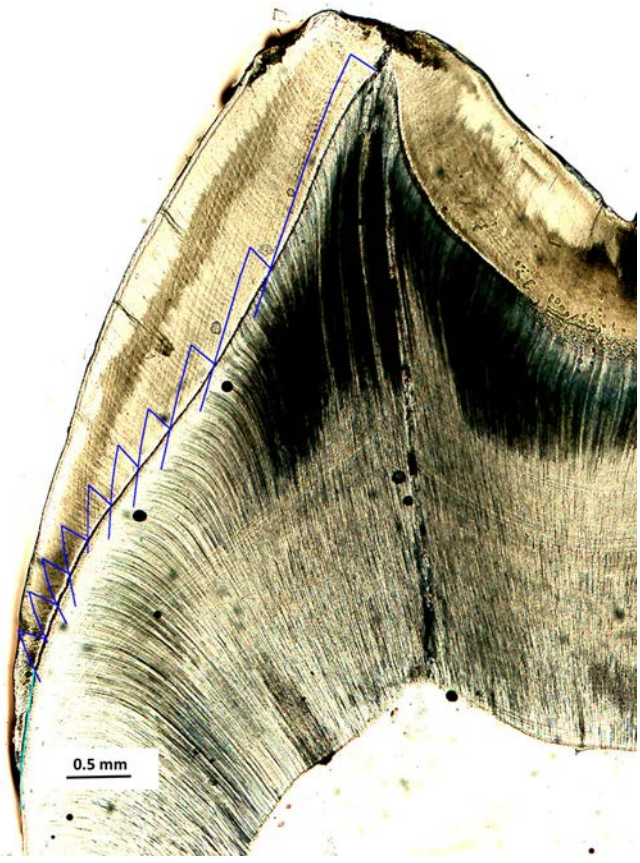

FIGURE 2 Zigzag method (Dean, 2009, 2012; Guatelli-Steinberg et al., 2012) of measuring EDJ lengths corresponding to 200 μm prism lengths shown in the buccal cusp of a *Cercocebus* upper second molar (specimen TF = 24–3). Each EDJ segment length was divided by the daily secretion rate in that region of the crown to obtain the enamel extension rate (EER). Note the small portion of the EDJ length (marked with a cyan line) on which it was not possible to apply this method. As noted in the text, the EER of the preceding segment was applied to this region and used in the calculation of overall enamel formation time. See text for additional details

4.4 | Statistical methods

Graphs were generated in SYSTAT version 13. Statistical analyses were carried out in SAS v. 9.4 (SAS Institute, 2015). Proc Mixed (the Mixed Procedure) was used to analyze differences between *Cercocebus* and *Lophocebus* in RET and ACS and was also used for the analysis of enamel growth variables. This procedure fits mixed linear models to

TABLE 3 Summary statistics by tooth type for RET, AET (mm.), BCD (mm.) and ACS for upper molar mesial and distal slices (mean ± 1SD)

Taxon	Slice	Tooth	*n*	RET	AET	BCD	ACS
C. atys	Mesial	UM1	7	12.4 ± 1.4	0.576 ± 0.07	7.6 ± 0.9	1.48 ± 0.15
		UM2	15	13.3 ± 1.6	0.715 ± 0.08	8.5 ± 0.7	1.74 ± 0.14
		UM3	12	14.8 ± 1.6	0.747 ± 0.05	8.1 ± 0.7	1.74 ± 0.09
		All uppers	34	13.6 ± 1.8	0.697 ± 0.09	8.2 ± 0.8	1.68 ± 0.16
	Distal	UM1	9	14.1 ± 1.7	0.565 ± 0.10	6.6 ± 1.1	1.37 ± 0.24
		UM2	14	15.1 ± 2.3	0.706 ± 0.09	7.9 ± 0.8	1.66 ± 0.16
		UM3	12	16.2 ± 2.0	0.712 ± 0.07	7.0 ± 1.0	1.60 ± 0.16
		All uppers	35	15.2 ± 2.1	0.672 ± 0.11	7.2 ± 1.1	1.60 ± 0.21
L. albigena	Mesial	UM1	4	15.8 ± 1.8	0.611 ± 0.08	6.3 ± 0.5	1.39 ± 0.10
		UM2	4	14.3 ± 0.7	0.627 ± 0.03	7.4 ± 0.4	1.52 ± 0.06
		UM3	4	15.7 ± 0.3	0.643 ± 0.04	6.7 ± 0.4	1.47 ± 0.07
		All uppers	12	15.3 ± 1.2	0.627 ± 0.05	6.8 ± 0.6	1.46 ± 0.09
	Distal	UM1	2	15.4 ± 1.3	0.591 ± 0.03	6.3 ± 0.4	1.37 ± 0.00
		UM2	3	15.9 ± 1.3	0.632 ± 0.03	6.8 ± 0.6	1.46 ± 0.04
		UM3	4	18.7 ± 2.6	0.643 ± 0.07	5.5 ± 0.8	1.30 ± 0.10
		All uppers	9	17.0 ± 2.3	0.628 ± 0.05	6.1 ± 0.9	1.37 ± 0.10
L. atterimus	Mesial	UM1	–	–	–	–	–
		UM2	1	14.8	0.649	6.5	1.45
		UM3	–	–	–	–	–
		All uppers	1	14.8	0.649	6.5	1.45
	Distal	UM1	–	–	–	–	–
		UM2	1	15.4	0.606	6.3	1.38
		UM3	–	–	–	–	–
		All uppers	1	15.4	0.606	6.3	1.38

Abbreviations: ACS, absolute crown strength; AET, average enamel thickness; BCD, bicervical diameter; RET, relative enamel thickness.

data, allowing a repeated measures analysis that was useful when using measurements from the same individual (e.g., more than one tooth type; more than one enamel extension rate measure). AET and tooth size were not analyzed statistically, as both are incorporated into ACS. The variables RET and ACS were modeled as a function of genus, tooth type, and the interaction of tooth type and genus. Each individual was treated as a subject with tooth type as the repeated measure. Models were run with four different variance–covariance structures and results from models with the lowest AICs are reported here. Since there were 4 ways to obtain significance for RET (for genus, and the genus by tooth type interaction, for upper and lower teeth), a Bonferroni-corrected alpha value of 0.0125 was used; for the same reason the alpha value used for ACS was 0.0125. Bootstrapped t-tests were used to compare the two genera in daily secretion rates, functional cusp flare, proportional linear basin occlusal enamel thickness, proportional maximum functional lateral enamel thickness, and crown shape. Bonferroni corrections were used given that there were multiple tests of the same variable. For example, there were four tests of DSR differences between *Cercocebus* and *Lophocebus*, so an alpha value of 0.05/4 (or 0.0125) was used in this comparison.

5 | RESULTS

5.1 | RET and ACS

Summary statistics by tooth type for RET, AET, and ACS are given for mesial and distal slices of upper molars in Table 3 and mesial and distal slices of lower molars in Table 4. To illustrate general trends, Figure 3 shows box plots of the upper and lower dentitions of *Cercocebus* and *Lophocebus* for mesial and distal slices for both RET and ACS. In general, there is a tendency for *Cercocebus* to have lower RET but greater ACS than *Lophocebus*. As can be seen in Tables 3 and 4, *Cercocebus* tends to have both greater AET and greater bi-cervical diameters.

Results are summarized in Table 5. Statistically significant RET and ACS differences were found for genus and/or the genus*tooth interaction for upper molars; this was not the case for lower molars, likely in part because of the smaller sample sizes available for these latter comparisons. The genus difference in RET for upper molars reflects the greater RET of *Lophocebus* relative to *Cercocebus*, while the genus difference in ACS for upper molars reflects the greater ACS of *Cercocebus* compared to *Lophocebus*.

TABLE 4 Summary statistics by tooth type for RET, AET (mm.), BCD (mm.) and ACS for mesial and distal slices of lower molars (mean ± 1SD)†

Taxon	Slice	Tooth	*n*	RET	AET	BCD	ACS
C. atys	Mesial	LM1	4	12.2 ± 0.8	0.526 ± 0.04	5.9 ± 0.8	1.24 ± 0.13
		LM2	2	12.0 ± 0.8	0.680 ± 0.01	7.8 ± 0.0	1.63 ± 0.01
		LM3	5	14.5 ± 1.6	0.732 ± 0.04	7.3 ± 0.7	1.74 ± 0.09
		All lowers	11	13.2 ± 1.7	0.648 ± 0.10	6.9 ± 1.0	1.49 ± 0.21
	Distal	LM1	2	13.1 ± 2.7	0.499 ± 0.14	5.2 ± 0.9	1.13 ± 0.25
		LM2	1	14.1	0.704	7.5	1.62
		LM3	4	15.8 ± 1.7	0.755 ± 0.08	6.7 ± 0.9	1.59 ± 0.16
		All lowers	7	14.8 ± 2.1	0.674 ± 0.15	6.4 ± 1.1	1.46 ± 0.27
L. albigena	Mesial	LM1	4	16.3 ± 2.5	0.584 ± 0.07	5.2 ± 0.5	1.23 ± 0.08
		LM2	4	15.4 ± 0.8	0.656 ± 0.06	6.5 ± 0.4	1.46 ± 0.11
		LM3	3	14.4 ± 1.0	0.602 ± 0.06	6.3 ± 0.4	1.38 ± 0.08
		All lowers	11	15.5 ± 1.7	0.615 ± 0.07	6.0 ± 0.7	1.35 ± 0.13
	Distal	LM1	–	–	–	–	–
		LM2	2	14.8 ± 1.9	0.632 ± 0.03	6.8 ± 0.6	1.48 ± 0.15
		LM3	2	18.7 ± 1.9	0.660 ± 0.01	4.7 ± 1.1	1.46 ± 0.04
		All lowers	4	16.8 ± 2.6	0.626 ± 0.04	6.1 ± 2.0	1.36 ± 0.18

Abbreviations: ACS, absolute crown strength; AET, average enamel thickness; BCD, bicervical diameter; RET, relative enamel thickness.

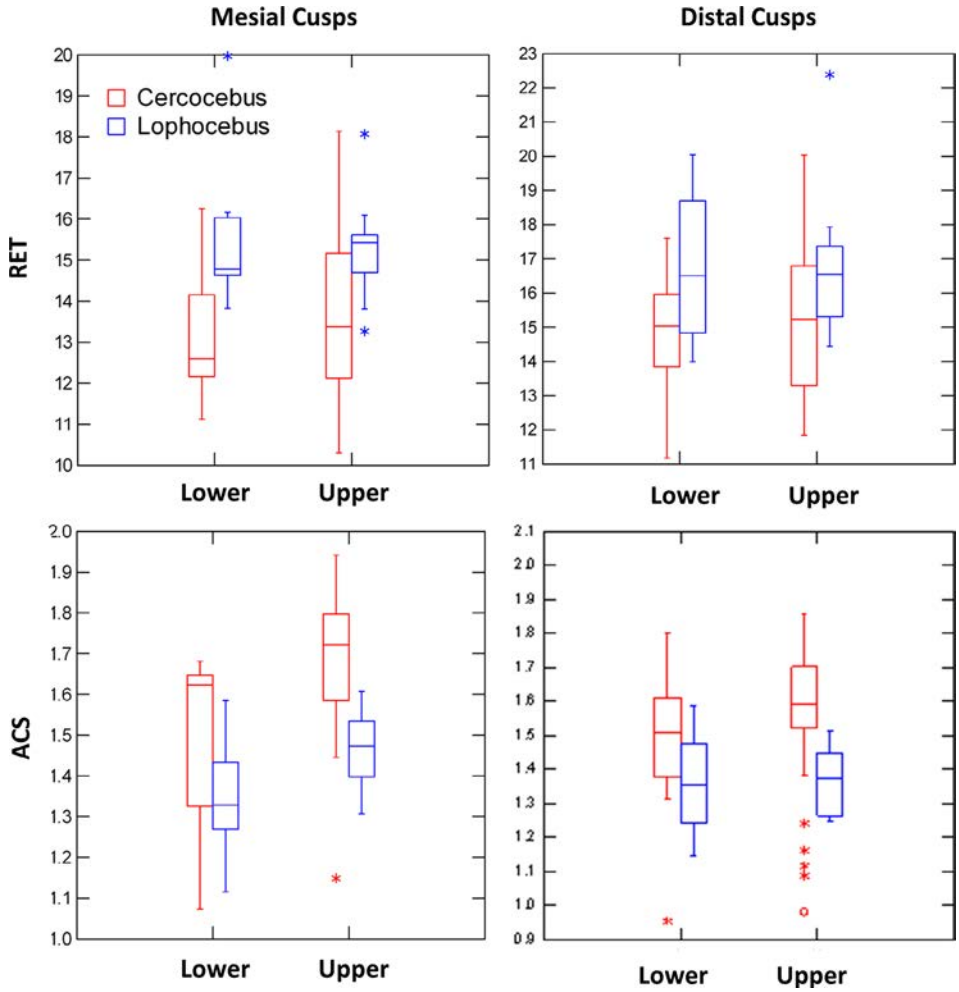

FIGURE 3 Box plots comparing *Cercocebus* and *Lophocebus* for RET and ACS for mesial and distal cusp µCT slices for all upper molars combined and all lower molars combined

TABLE 5 Proc mixed results for Mesial cusps

Variable	Model significance	Effect	Numerator df	Denominator df	*F* value	*p* Value
Upper RET	***p* < 0.0015**					
		Tooth	2	15	10.90	**0.0012**
		Genus	1	26	8.29	**0.0079**
		Tooth*Genus	2	15	8.37	**0.0036**
Lower RET	*p* < 0.1618					
		Tooth	2	5	0.15	0.8662
		Genus	1	11	8.70	0.0132
		Tooth*Genus	2	5	5.07	0.0627
Upper ACS	***p* < 0.0163**					
		Tooth	2	15	17.61	**0.0001**
		Genus	1	26	12.15	**0.0018**
		Tooth*Genus	2	15	4.43	0.0308
Lower ACS	***p* < 0.0166**					
		Tooth	2	5	46.98	**0.0006**
		Genus	1	11	4.61	0.0550
		Tooth*Genus	2	5	5.52	0.0543

Note: Boldface denotes statistical significance.

TABLE 6 Descriptive statistics for proportional occlusal basin linear enamel thickness and proportional functional cusp linear enamel thickness in mm (mean ± 1SD)

Taxon	Tooth	Proportional occlusal basin linear enamel thickness (*n*)	Proportional functional cusp linear enamel thickness (*n*)
C. atys	UM1	–	1.359 ± 0.196 (8)
	UM2	1.535 ± 0.170 (8)	1.569 ± 0.233 (13)
	UM3	1.429 ± 0.120 (8)	1.519 ± 0.132 (13)
	All uppers	1.479 ± 0.148 (17)	1.501 ± 0.203 (34)
	LM1	1.690 ± 0.043 (2)	1.492 ± 0.096 (4)
	LM2	1.198 (1)	1.439 ± 0.027 (2)
	LM3	1.556 ± 0.133 (4)	1.534 ± 0.080 (5)
	All lowers	1.543 ± 0.191 (7)	1.501 ± 0.082 (11)
L. albigena	UM1	–	1.294 ± 0.216 (4)
	UM2	1.227 ± 0.470 (2)	1.445 ± 0.105 (5)
	UM3	1.041 ± 0.096 (2)	1.499 ± 0.086 (4)
	All uppers	1.134 ± 0.297 (4)	1.415 ± 0.158 (13)
	LM1	–	1.293 ± 0.156 (4)
	LM2	0.965 (1)	1.497 ± 0.041 (4)
	LM3	1.027 ± 0.153 (2)	1.693 ± 0.196 (3)
	All lowers	1.007 ± 0.114 (3)	1.476 ± 0.208 (11)

Notes: The word "proportional" refers to the scaling of a linear enamel thickness measurement to AET. Proportional occlusal basin linear thickness is defined as the ratio of the linear thickness of the occlusal basin to AET. Proportional functional cusp linear enamel thickness is defined as the ratio of the functional cusp linear thickness to AET. Numbers greater than 1 represent linear enamel thickness in a region that exceeds the AET of a crown.

5.2 | Enamel thickness distribution

Measurements on occlusal basins could only be performed on completely unworn molars and maximum functional cusp wall linear thickness required molars with intact dentine horns. For these reasons, the data are limited across tooth types (Table 6). Figure 4 compares the two genera for proportional linear occlusal basin thickness and proportional maximum linear functional cusp wall enamel thickness and Table 7 reports the results of bootstrapped t-tests for these variables. For these tests, to optimize sample sizes, second and third molars for each jaw were combined. First molars were omitted since they were less well balanced across the two genera.

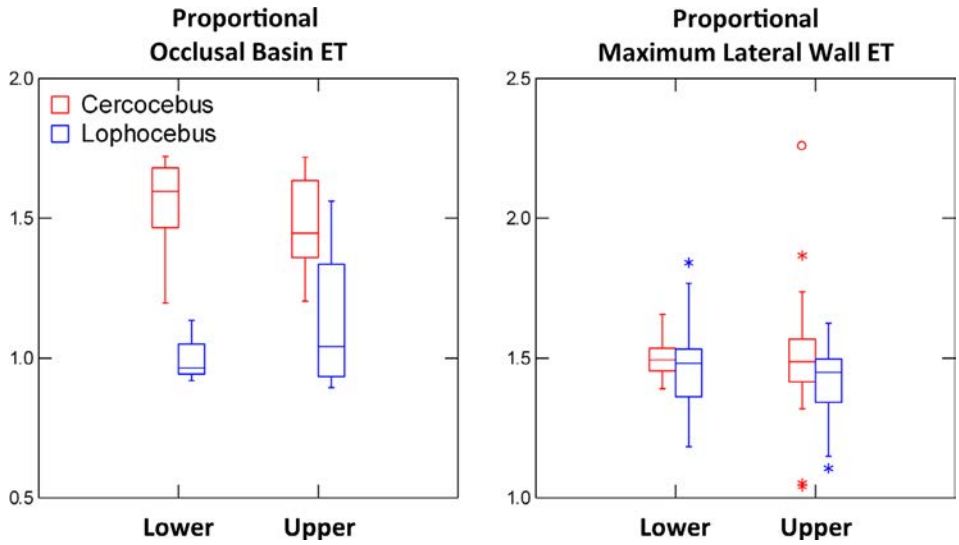

FIGURE 4 Box plots comparing *Cercocebus* and *Lophocebus* for mesial cusp mCT slices for proportional linear occlusal basin enamel thickness (ET) and proportional lateral wall maximum enamel thickness (ET)

TABLE 7 Results of bootstrapped *t*-tests for proportional occlusal basin linear enamel thickness and proportional functional wall linear enamel thickness

Variable	Jaw	*Cercocebus* (*n*)	*Lophocebus* (*n*)	Variances	Df	*T* value	*p*-Value
Proportional Occlusal Basin ET	Upper	16	4	Equal	18	3.37	**0.0030**
	Lower	5	3	Equal	6	3.76	**0.0094**
Proportional Functional Wall ET	Upper	26	9	Equal	33	1.15	0.2604
	Lower	7	7	Equal	12	−1.11	0.2908

Abbreviations: ET, enamel thickness.
Note: Boldface denotes statistical significance.

TABLE 8 Summary statistics for enamel growth variables for upper molars (mean ± 1SD)

	n	Occlusal basin DSR (days per μm)	Cuspal DSR (days per μm)	Mid-crown DSR (days per μm)	Cervical DSR (days per μm)	Initial EER (μm/day)	Enamel formation time (days)
Lingual cusp							
Cercocebus	8	3.9 ± 0.4	3.7 ± 0.4	4.1 ± 0.1	3.5 ± 0.3	40.2 ± 5.1	738 ± 69
Lophocebus	2	4.2 ± 0.5	4.5 ± 0.4	3.9 ± 0.4	3.2 ± 0.3	29.5 ± 9.6	662 ± 69
Buccal cusp							
Cercocebus	12	3.9 ± 0.3	3.7 ± 0.3	4.1 ± 0.3	3.6 ± 0.4	32.4 ± 5.3	626 ± 82
Lophocebus	4	4.3 ± 0.6	4.01 ± 0.2	4.2 ± 0.4	3.3 ± 0.3	22.7 ± 2.0	571 ± 80

Abbreviations: DSR, daily secretion rate; EER, enamel extension rate.

Proportional occlusal basin thickness is significantly greater for *Cercocebus* than it is for *Lophocebus*, while the two genera do not differ significantly in proportional maximum linear functional cusp wall enamel thickness.

5.3 | Enamel growth variables

Summary statistics for upper molar (Upper M2 and Upper M3 mesial slices) enamel growth variables are given in Table 8.

Bootstrapped *t*-tests were performed for the "nonfunctional" buccal cusps, for which we had the largest sample: 12 *Cercocebus* and 4 *Lophocebus*. For DSRs, four tests were performed, with a Bonferroni-corrected alpha of 0.0125. None of the DSR differences between *Cercocebus* and *Lophocebus* were statistically significant at either the 0.0125 of 0.05 levels. Nonfunctional cusp enamel formation time (in days) was also not statistically significantly different between the two genera ($p < 0.2689$), although the two genera differed significantly in nonfunctional cusp EDJ length ($p < 0.0006$), with *Cercocebus* having greater EDJ length than *Lophocebus*. Thus, although the two genera differ significantly in EDJ length for their functional cusps, they do not have a statistically significant difference in their enamel formation times (although as can be seen in Table 8, numerically, *Lophocebus* has slightly shorter enamel formation times). This finding suggests that the longer EDJ lengths of *Cercocebus* are forming at a faster rate. This possibility is explored in the growth curve analysis of enamel extension rates.

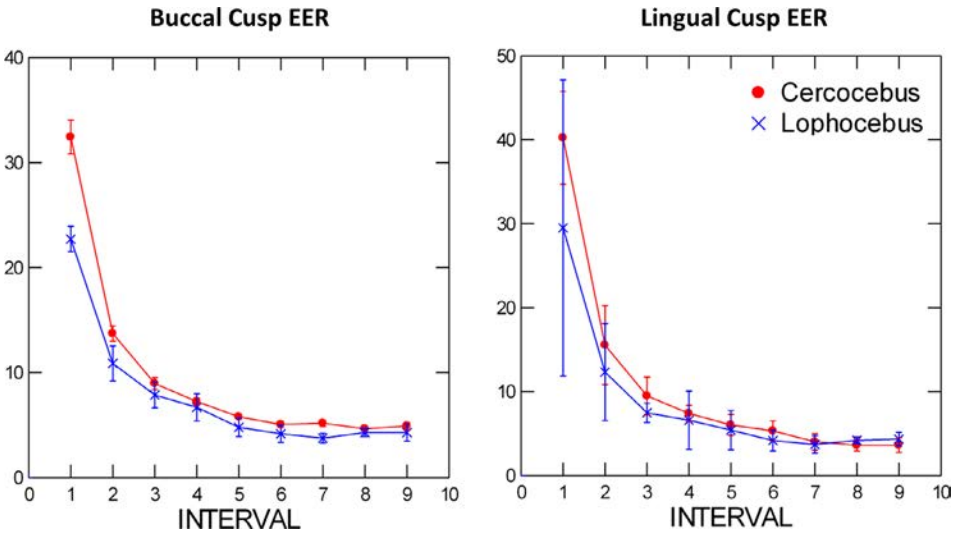

FIGURE 5 Mean ± 1SD enamel extension rates (EER) (μm/day) on nonfunctional (buccal) cusps and functional (lingual) cusps for upper second and third molars. Note that *Cercocebus* starts at a much higher rates than *Lophocebus* and maintains a slightly higher rate at most later time intervals. That is the basis for the significant effect of genus and the interaction of genus and interval in the mixed linear model results

TABLE 9 Analysis of nonfunctional cusp enamel extension rates (EERs)

Effect	Numerator df	Denominator df	*F* value	*p* Value
Interval	1	14	281.49	**<0.0001**
Genus	1	107	9.54	**0.0026**
Interval*Genus	1	107	5.4	**0.0220**
Interval*Interval	1	107	178.3	**<0.0001**

Note: Boldface denotes statistical significance.

Growth curves were modeled in Proc Mixed for upper second and third molars combined for buccal (nonfunctional) cusps. Sample sizes were too small for statistical comparison for the lingual (functional) cusps; however, both nonfunctional and functional cusp data are plotted in Figure 5.

For the Proc Mixed growth comparison of nonfunctional cusps, there were two M2s and two M3s for *Lophocebus* and seven M2s and five M3s, for *Cercocebus*. The first nine enamel extension rate measures (interval 1 through interval 9) were treated as repeated measures for each individual, modeled as a quadratic, with the null model likelihood tests statistically significant ($p < 0.0254$). Individual variation was treated as a random effect. One individual had two molars in this test; the rest were represented by a single molar each. Tests for interval and genus are shown in Table 9. All predictors were statistically significant, including genus and the interval*-genus predictors, indicating that the growth curves of these species differ. This difference can be seen in Figure 5, which plots mean enamel extension rates for upper and lower molars. Note that *Cercocebus* starts at a much higher rates than *Lophocebus* and maintains a slightly higher rate at most later time intervals. That is the basis for the significant effect of genus and the interaction of genus and interval.

5.4 | Cusp tip geometry and molar flare

Measurements on cusp tips could only be performed on completely unworn molars, while functional cusp flare required molars with intact dentine horns. Table 10 provides descriptive statistics for cusp tip angle and functional cusp flare in degrees.

As there were very few specimens with completely unworn functional cusp tips, no statistical comparisons were attempted for this variable, although Figure 6 suggests a tendency for *Cercocebus* to have sharper cusps than *Lophocebus*. For functional cusp flare, second and third molars for each jaw were combined to optimize sample sizes for bootstrapped t-tests comparing *Cercocebus* and *Lophocebus*. First molars were omitted since they were not well balanced across the two genera. There were two *t*-tests performed (upper and lower dentitions), so an alpha value of 0.025 was used. Table 11 summarizes results of the t-tests for molar flare. There was a statistically significant difference between these genera in functional cusp flare for lower molars, with *Cercocebus* exhibiting greater flare, but no significant difference was found for upper molars.

6 | DISCUSSION AND CONCLUSION

This study investigated the hypothesis that compared to the molars of *Lophocebus*, *Cercocebus* molars would possess features that afford them greater resistance to fracture, and that these features would have underlying enamel growth correlates. This hypothesis was partially supported by our analyses (see Table 12). The functionally relevant features of molar anatomy that supported our hypothesis were the following: *Cercocebus* exhibited greater values of ACS (upper molars), functional cusp flare (lower molars), and proportional occlusal basin enamel thickness (both upper and lower molars). At the same

TABLE 10 Descriptive statistics for cusp tip angle and functional cusp flare in degrees (mean ± 1SD)

Taxon	Tooth	Functional cusp tip angle (*n*)	Functional cusp flare (*n*)
C. atys	UM1	100.0 (1)	28.5 ± 5.1 (6)
	UM2	88.1 ± 12.0 (8)	28.4 ± 3.6 (13)
	UM3	89.5 ± 8.1 (8)	29.3 ± 4.0 (12)
	All uppers	89.5 ± 10.0 (17)	28.7 ± 4.0 (31)
	LM1	92.0 ± 6.4 (2)	31.9 ± 6.5 (4)
	LM2	68.5 (1)	39.9 ± 1.6 (2)
	LM3	92.8 ± 7.7 (3)	36.1 ± 4.3 (5)
	All lowers	88.5 ± 11.3 (6)	35.3 ± 5.4 (11)
L. albigena	UM1	–	32.3 (1)
	UM2	111.4 (1)	28.5 ± 1.9 (4)
	UM3	98.7 (1)	25.8 ± 2.5 (4)
	All uppers	105.1 ± 9.0 (2)	27.7 ± 2.9 (9)
	LM1	–	–
	LM2	–	34.4 ± 1.94 (2)
	LM3	99.5 (1)	27.4 ± 2.65 (3)
	All lower	99.5 (1)	30.2 ± 4.4 (5)

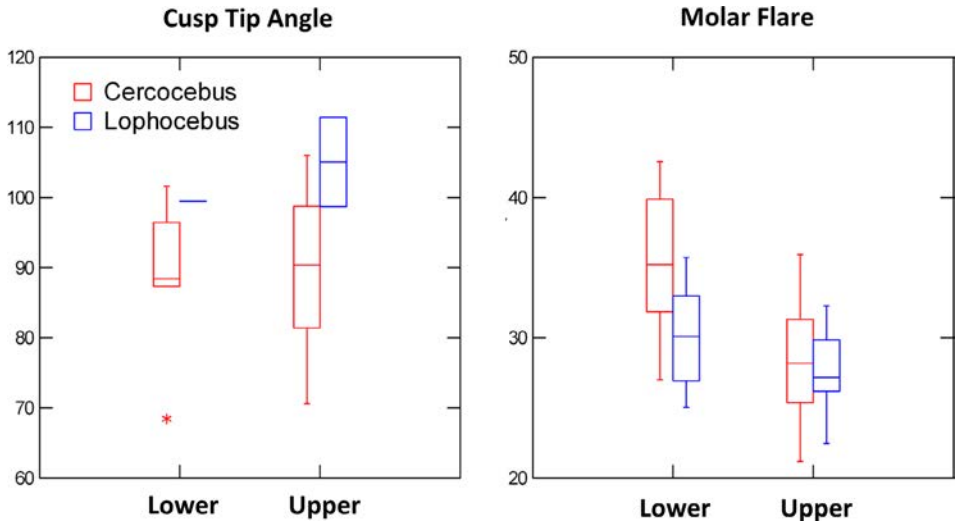

FIGURE 6 Box plots comparing *Cercocebus* and *Lophocebus* for mesial cusp mCT slices for cusp tip angles and molar flare

TABLE 11 Results of bootstrapped *t*-tests for functional cusp flare

Variable	Jaw	*Cercocebus* (*n*)	*Lophocebus* (*n*)	Variances	Df	*T* value	*p*-Value
Functional cusp flare	Upper	25	8	Equal	31	1.16	0.2568
	Lower	7	5	Equal	10	2.88	**0.0165**

Note: Boldface denotes statistical significance.

time, *Cercocebus* possessed lower RET values than *Lophocebus* and displayed a tendency to exhibit sharper cusp tips (there were, however, insufficient sample sizes to perform statistical tests for this feature). Proportional functional lateral wall enamel thickness did not differ significantly between the two genera. Some of the differences between the molars of *Cercocebus* and *Lophocebus* can be seen in the μCT images shown in Figure 7.

In terms of enamel growth, no significant differences were found between genera in enamel daily secretion rates or crown formation times; however, extension rates in *Cercocebus* were significantly greater than they were in *Lophocebus*. *Cercocebus* had significantly longer EDJ lengths than *Lophocebus* and therefore appears to grow its longer EDJs primarily through faster rates of enamel extension rather than by significantly prolonging crown formation time. These functional and enamel growth details appear consistent with one another: larger (both taller and wider) crowns that are not significantly different in daily enamel secretion rates and crown formation time could be expected to have lower RET, all other factors being equal.

TABLE 12 Summary of results relative to predictions

Feature	Prediction	Lower molar results	Upper molar results
Relative enamel thickness (RET)	*Cercocebus* *Lophocebus*	***Cercocebus* *Lophocebus*** **Supported**	*Cercocebus* < *Lophocebus* Not supported
Absolute crown strength (ACS)	*Cercocebus* > *Lophocebus*	*Cercocebus* *Lophocebus* Not supported	***Cercocebus* > *Lophocebus*** **Supported**
Occlusal basin thickness (OBT)	*Cercocebus* > *Lophocebus*	***Cercocebus* > *Lophocebus*** **Supported**	***Cercocebus* > *Lophocebus*** **Supported**
Lateral wall enamel thickness (LWET) of functional cusps	*Cercocebus* > *Lophocebus*	*Cercocebus* *Lophocebus* Not supported	*Cercocebus* *Lophocebus* Not supported
Enamel growth variables: DSR and crown formation time	*Cercocebus* ≠ *Lophocebus*	Not evaluated	*Cercocebus* *Lophocebus* Not supported
Enamel growth variables: EER	*Cercocebus* ≠ *Lophocebus*	Not evaluated	***Cercocebus* > *Lophocebus*** **Supported**
Cusp angle	*Cercocebus* > *Lophocebus*	*Cercocebus* might be less blunt Unclear	*Cercocebus* might be less blunt Unclear
Flare of functional cusps	*Cercocebus* > *Lophocebus*	***Cercocebus* > *Lophocebus*** **Supported**	*Cercocebus* *Lophocebus* Not supported

Note: Boldface denotes statistical significance.

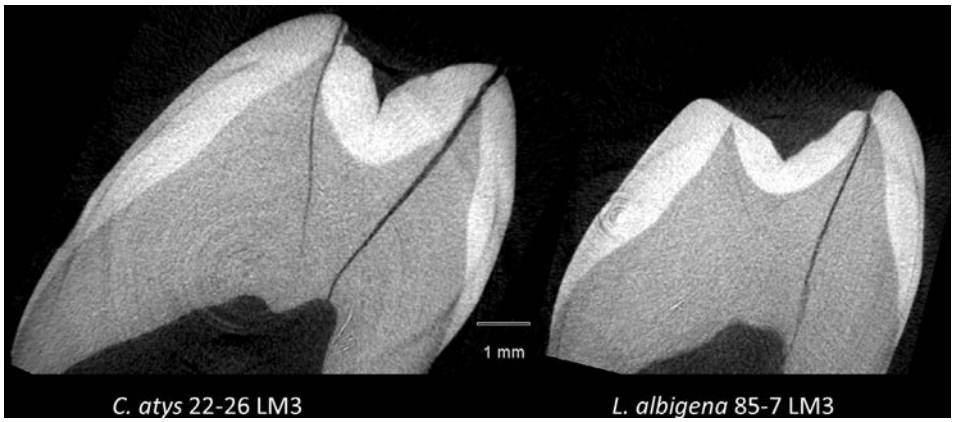

FIGURE 7 *C. atys* (specimen 22–26) lower third molar on the left vs. *L. albigena* (specimen 85–7) lower third molar on the right. The buccal (functional) side of the tooth is on the left in each image. Note the greater flare of the *C. atys* molar (elongated buccal side of the crown), which results in a greater dentine-core area than that of *L. albigena*. Also note the thickened occlusal basin enamel in the *C. atys* molar relative to that of *L. albigena*

Not all features of *Cercocebus* molars appear to provide greater fracture resistance than those of *Lophocebus*. This finding begs the question of whether it is the combination of features within each genus that might produce differences in how well their molars resist fracture. To address this question, molars with the features described here could be modeled using finite element analysis to assess their performance under a variety loading of loading regimes (e.g., Kupczik & Lev-Tov Chattah, 2014). Furthermore, this study only examined molars, yet premolars are obviously involved in mastication as well, and the P4s of *Cercocebus* are larger relative to their first molars than those of *Lophocebus* (Fleagle & McGraw, 1999). Few of the features examined in the present molar study have which been explored in mangabey premolars. Lastly, decussation, the crisscrossing of enamel prisms that resists crack propagation (Bajaj et al., 2008), was not examined in the present study. Comparison of the two mangabey genera in terms of degree of decussation would also be relevant to fully understanding how their molars resist fracture and might be especially relevant to the problem of fatigue stress (Gao et al., 2016).

Nevertheless, the fact remains that both genera can and do eat very hard objects. The present investigation aligns with what recent studies have suggested: there is more than one way to crack obdurate foods (Constantino et al., 2011; Thiery et al., 2017; van Casteren et al., 2019). Sea otters (*Enhydra lutris*) crack the shells of clams, mussels, and abalone with thin enameled but large, bunodont molars (Constantino et al., 2011). In Loango National Park, Gabon, western lowland gorillas (*Gorilla gorilla*), whose molars have thin enamel, consume hard seeds of *Coula edulis* throughout its annual fruiting season. In both of these mammals, large overall tooth size appears to compensate for relatively thin enamel. Indeed, despite their relatively thin enamel, gorillas have the highest ACS values among all living hominoids (Schwartz et al., 2020). It is therefore conceivable that for *Cercocebus* and *Lophocebus*, a similar dynamic is at work, such that the larger teeth of *Cercocebus*, which have greater ACS than *Lophocebus*, do not require relatively thicker enamel. In a reciprocal fashion, the relatively thicker enamel of *Lophocebus* molars may compensate for smaller size.

Proportionally thick occlusal enamel in *Cercocebus* relative to *Lophocebus* suggests that the former is better protected against fracture in this region of the tooth. An uneven distribution of enamel was predicted for primates consuming durophagous, as opposed to

abrasive diets (Lucas et al., 2008), and is associated with durophagy in cercopithecoids (Thiery et al., 2017). Moreover, as previously noted, proportionally thicker occlusal basin enamel, specifically, has been found in orangutans (Kono, 2004) and other durophagous primates (O'Hara, 2021). We note that despite the differences between *Cercocebus* and *Lophocebus* in occlusal basin enamel thickness, there was no difference between the two genera in daily enamel secretion rates in this region. Thickened enamel in the occlusal basin of *Cercocebus* must be produced by some other mechanism, such as by an increase in ameloblast lifespan (e.g., Grine & Martin, 1988) or other complex mechanisms related to the diffusion-limited secretion of enamel matrix atop the underlying dentine core (e.g., Häkkinen et al., 2019).

The greater functional cusp flare of *Cercocebus* lower molars might better buttress them against laterally-directed bite forces (Macho & Shimizu, 2009; Shimizu, 2002). Functional cusp flare in cercopithecoids appears to have evolved through the incorporation of the cingulum into the molar sidewall (Strasser & Delson, 1987). Molar flare is an ancient feature of Cercopithecoidea, present in the 22 Ma nonbilophodont stem Cercopithecoid *Alophia*, and becoming more pronounced in victoriapithecids in conjunction with increased bilophodonty, around 15.5 Ma (Rasmussen et al., 2019). Bilophodonty has been suggested to have originated in a seed-eating context, with the lophs acting as wedges (as per Lucas & Teaford, 1994) to initiate cracks in hard food items (Benefit, 1999). The apparent co-evolution of bilophodonty and well-developed molar flare in victoriapithecids supports the notion that both features originated within the context of durophagy.

Functional lateral cusp flare might also be linked to more pointed molar cusps, characteristic of Papionini relative to Cercopithecini (Kim, 2019). Perhaps greater molar flare is the reason why the cusps of *Cercocebus* tend to be more pointed than those of *Lophocebus*. Molar flare has also been suggested to relate to occlusal enamel thickness in that when cusp tips are narrowly spaced on a crown, the occlusal basin is constricted, arguably leading to the accumulation of thicker enamel during development in this region (Olejniczak et al., 2003). Figure 8 is a scatterplot of proportional linear occlusal basin thickness vs. functional cusp flare in mesial slices of *Cercocebus* and *Lophocebus* upper molars (all molar types combined). There does not appear to be a positive relationship between the two variables (if there is any relationship, it appears negative in this plot), but larger samples of each tooth type are required to address this question definitively. We note that the one *Lophocebus* molar with high proportional linear occlusal basin thickness belongs to *L. aterrimus*, perhaps indicating that there may be differences in this feature among *Lophocebus* species.

Despite possessing lower RET, *Cercocebus* molars have greater ACS than *Lophocebus* molars, supporting the hypothesis that overall, *Cercocebus* molars are better protected against fracture. The greater ACS and lower RET of *Cercocebus* may both be related to its greater flare. With more pronounced flare, *Cercocebus* molars are wider, and therefore have both greater coronal dentine areas and longer BCDs (Tables 3 and 4; Figure 7). Given that AET is scaled to coronal dentine area in calculating RET, greater molar flare would tend to cause RET to decrease. On the other hand, by increasing the bicervical diameter

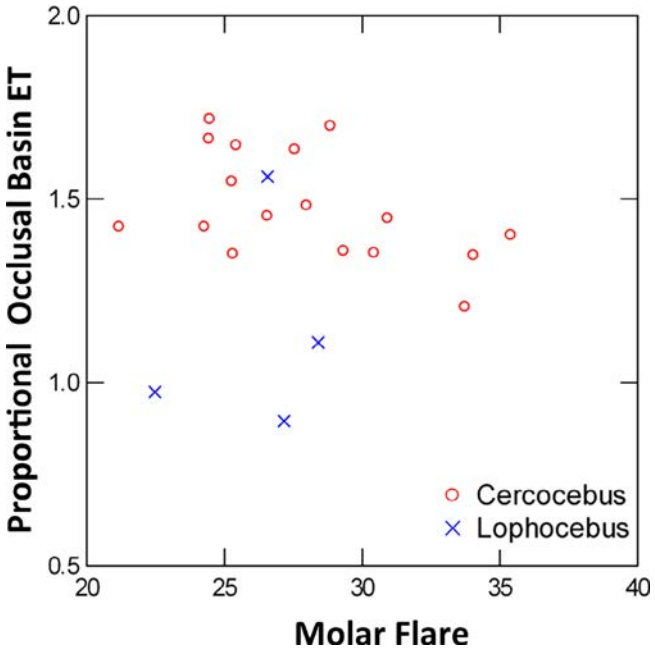

FIGURE 8 Scatterplot of proportional linear occlusal basin enamel thickness (ET) and functional cusp flare in *Cercocebus* and *Lophocebus* upper molar mesial slices

of a molar, greater flare would tend to cause ACS to increase. Essentially, greater flare, as occurs in *Cercocebus* relative to *Lophocebus* molars, may entail a trade-off between ACS and RET.

The data presented here suggest that taller teeth of *C. atys* are formed primarily by increasing the rate of enamel extension, rather than the duration of enamel formation. Given that taller crowns can result from either faster rates of enamel extension, by lengthening the crown formation period, or both (Guatelli-Steinberg et al., 2012), it may be significant from a life-history perspective that *C. atys* molars extend at faster rates than those of *Lophocebus*. Two studies have found correlations between enamel-formation front angles, which are associated with rates of enamel extension, and life history variables, brain size, and/or body size across a range of primates (Guatelli-Steinberg et al., 2018; Hogg & Walker, 2011).

According to the Food Processing Hypothesis (Godfrey et al., 2001), food mechanical properties can directly select for rates of dental development. Specifically, this hypothesis predicts that folivores should have more advanced dental emergence schedules than frugivores because folivorous weanlings must be dentally endowed enough to process mechanically challenging leaves and/or seeds. Harvati (2000) found that colobines, which are folivorous, have relatively advanced M2 and M3 emergence compared to other catarrhines. There is evidence that seed-eating folivores have even more accelerated emergence schedules than those that do not include seeds in their diets (Bolter, 2004). Relative to nonseed eaters, seed-eating folivores (*Presbytis rubicunda*, *Colobus angolensis*, and *Colobus satanas*) emerge their the M2s and M3s earlier in their emergence sequences (Bolter, 2004). It would be interesting to know if other aspects of *Cercocebus* dental growth and development—besides their rates of

enamel extension—are accelerated relative to *Lophocebus*. Even newly weaned sooty mangabeys are capable of cracking hard *Sacoglottis* seed casings (McGraw et al., 2011), perhaps indicating that selection has targeted accelerated dental development in this taxon, although selection for accelerated dental development might also reflect more global influences (e.g., predation pressure) on the pace of *Cercocebus* growth and development. Additional research aimed at elucidating relationships among dental development, masticatory mechanics, and the ontogeny of ecological independence would provide an avenue for testing the application of the Food Processing Hypotheses to mangabeys.

7 | CONCLUSION

Cercocebus and *Lophocebus* are both known hard-object feeders, but the former eats hard foods more regularly than the latter. With a greater frequency of hard-food mastication, *Cercocebus* was hypothesized to have molars with features that would endow them with greater fracture resistance than those of *Lophocebus*, a fallback consumer of hard foods. This study compared RET, ACS, proportional linear occlusal basin thickness, functional lateral wall thickness, functional cusp tip angles and functional cusp lateral flare between molars of the two genera. Although some comparisons revealed no statistically significant differences between the two genera, *Cercocebus* molars were shown to have significantly greater ACS (upper molars only), proportional linear occlusal basin thickness (both upper and lower molars), and molar flare (lower molars only), consistent with greater fracture resistance. However, *Cercocebus* had significantly lower RET (upper molars only) than *Lophocebus*. We suggest that greater molar flare in *C. atys* contributes to its greater ACS and lower RET relative to *Lophocebus* by increasing its bi-cervical diameter and dentine core area. We further argue that because ACS is a better predictor than RET of the fracture resistance of a tooth (Schwartz et al., 2020), *C. atys* molars appear to be more fracture resistant than those of *Lophocebus*. Finally, we also examined aspects of enamel growth in these molars, finding that the larger (and taller) crowns of *C. atys* extended in height significantly more rapidly than those of *Lophocebus* but did not form in significantly shorter periods of time.

AUTHOR CONTRIBUTIONS

Debbie Guatelli-Steinberg: Conceptualization (lead); data curation (lead); formal analysis (lead); funding acquisition (lead); investigation (equal); methodology (equal); project administration (lead); resources (equal); software (equal); supervision (lead); validation (lead); visualization (lead); writing – original draft (lead); writing – review and editing (equal). **Gary T. Schwartz:** Conceptualization (supporting); funding acquisition (supporting); investigation (supporting); writing – review and editing (equal). **Mackie C. O'Hara:** Conceptualization (supporting); data curation (supporting); funding acquisition (supporting); investigation (supporting); methodology (supporting); software (lead); validation (supporting); writing – review and editing (equal). **Kaita Gurian:** Data curation (supporting); investigation (supporting); methodology (supporting); supervision (supporting); validation (supporting). **Jess Rychel:** Data curation (supporting); investigation (supporting). **W. Scott McGraw:** Conceptualization (equal); data curation (supporting); formal analysis (supporting); funding acquisition (equal); investigation (equal); project administration (supporting); writing – review and editing (equal).

ACKNOWLEDGMENTS

This project was funded by NSF grant 1945008 to Debbie Guatelli-Steinberg, W. Scott McGraw, and Gary T. Schwartz. The authors thank our undergraduate tooth extraction team: Gina De Marsh, Ryan Phelan, and Ellie Sarle. Special thanks to Jie Liu for her advice and assistance with μCT scanning and to and Do-Gyoon Kim for use of the scanner in his lab. The authors also thank Brian Foster and Michael Chavez for an introduction to μCT scanning. Leigh Oldershaw helped with the initial inventory of specimens. Finally, the authors thank Kate McGrath, Don Reid, Shannon McFarlin, Patrick Mahoney, and Rebecca Ferrell for advice on enamel histology.

CONFLICT OF INTEREST

The authors have no conflicts of interest.

DATA AVAILABILITY STATEMENT

The data that support the findings of this study are available from the corresponding author upon reasonable request.

ORCID

Debbie Guatelli-Steinberg https://orcid.org/0000-0002-1345-5384
Gary T. Schwartz https://orcid.org/0000-0003-4428-2102
Mackie C. O'Hara https://orcid.org/0000-0002-1221-0668

REFERENCES

Almotairy, N., Kumar, A., & Grigoriadis, A. (2021). Effect of food hardness on chewing behavior in children. *Clinical Oral Investigations*, *25*(3), 1203–1216.

Bajaj, D., Nazari, A., Eidelman, N., & Arola, D. D. (2008). A comparison of fatigue crack growth in human enamel and hydroxyapatite. *Biomaterials*, *29*(36), 4847–4854.

Benefit, B. R. (1999). *Victoriapithecus*: The key to Old World monkey and catarrhine origins. *Evolutionary Anthropology: Issues, News, and Reviews: Issues, News, and Reviews*, *7*(5), 155–174.

Bolter, D. R. (2004). *Anatomical growth patterns in colobine monkeys and implications for primate evolution*. University of California, Santa Cruz.

Brugiere, D., Gautier, J.-P., Moungazi, A., & Gautier-Hion, A. (2002). Primate diet and biomass in relation to vegetation composition and fruiting phenology in a rain forest in Gabon. *International Journal of Primatology*, *23*, 999–1024.

Constantino, P. J., Lee, J. J. W., Morris, D., Lucas, P. W., Hartstone-Rose, A., Lee, W. K., Dominy, N. J., Cunningham, A., Wagner, M., & Lawn, B. R. (2011). Adaptation to hard-object feeding in sea otters and hominins. *Journal of Human Evolution*, *61*, 89–96.

Constantino, P. J., Lucas, P. W., Lee, J. J., & Lawn, B. R. (2009). The influence of fallback foods on great ape tooth enamel. *American Journal of Physical Anthropology*, *140*, 653–660.

Cronin, J. E., & Sarich, V. M. (1976). Molecular evidence for dual origin of mangabeys among Old World monkeys. *Nature*, *260*, 700–702.

Daegling, D. J., McGraw, W. S., Ungar, P. S., Pampush, J. D., Vick, A. E., & Bitty, E. A. (2011). Hard-object feeding in sooty mangabeys

(*Cercocebus atys*) and interpretation of early hominin feeding ecology. *PLoS One*, *6*(8), e23095.

Dean, M. C. (2009). Extension rates and growth in tooth height of modern humans and fossil hominin canines and molars. In T. Koppe & K. W. Alt (Eds.), *Comparative Dental Morphology* (Vol. 13, pp. 68–70). Karger.

Dean, M. C. (2012). A histological method that can be used to estimate the time taken to form the crown of a permanent tooth. In L. S. Bell (Ed.), *Forensic Microscopy for Skeletal Tissues: Methods and Protocols*, *Methods in Molecular Biology* (Vol. 915). Springer Science and Business Media, LLC.

Disotell, T. R. (1994). Generic level relationships of the Papionini (Cercopithecoidea). *American Journal of Physical Anthropology*, *94*(1), 47–57.

Fleagle, J. G., & McGraw, W. S. (1999). Skeletal and dental morphology supports diphyletic origin of baboons and mandrills. *Proceedings of the National Academy of Sciences*, *96*, 1157–1161.

Fleagle, J. G., & McGraw, W. S. (2002). Skeletal and dental morphology of African papionins: Unmasking a cryptic clade. *Journal of Human Evolution*, *42*, 267–292.

Gao, S. S., An, B. B., Yahyazadehfar, M., Zhang, D., & Arola, D. D. (2016). Contact fatigue of human enamel: Experiments, mechanisms and modeling. *Journal of the Mechanical Behavior of Biomedical Materials*, *60*, 438–450.

Godfrey, L. R., Samonds, K. E., Jungers, W. L., & Sutherland, M. R. (2001). Teeth, brains, and primate life histories. *American Journal of Physical Anthropology*, *114*(3), 192–214.

Grine, F. E., & Martin, L. B. (1988). Enamel thickness and development in Australopithecus and Paranthropus. In F. E. Grine (Ed.), *Evolutionary history of the 'Robust'Australopithecines* (pp. 3–42). Aldine de Gruyter.

Groves, C. P. (1978). Phylogenetic and population systematics of the mangabeys (primates: Cercopithecoidea). *Primates*, *19*, 1–34.

Groves, C. P. (2000). The phylogeny of the Cercopithecoidea. In P. F. Whitehead & C. J. Jolly (Eds.), *Old World monkeys* (pp. 77–98). Cambridge University Press.

Guatelli-Steinberg, D., Ferrell, R. J., Spence, J., Talabere, T., Hubbard, A., & Schmidt, S. (2009). Sex differences in anthropoid mandibular canine lateral enamel formation. *American Journal of Physical Anthropology*, *140*, 216–233.

Guatelli-Steinberg, D., Floyd, B. A., Dean, M. C., & Reid, D. (2012). Enamel extension rate patterns in modern human teeth: Two approaches designed to establish an integrated comparative context for fossil primates. *Journal of Human Evolution*, *63*, 475–486.

Guatelli-Steinberg, D., Pampush, J. D., O'Hara, M. C., Xing, S., McGraw, W. S., & Ferrell, R. J. (2018). Do mid-crown enamel formation front angles reflect factors linked to the pace of primate growth and development? *The Anatomical Record*, *301*(1), 125–139.

Häkkinen, T. J., Sova, S. S., Corfe, I. J., Tjäderhane, L., Hannukainen, A., & Jernvall, J. (2019). Modeling enamel matrix secretion in mammalian teeth. *PLoS Computational Biolology*, *15*(5), e1007058.

Ham, R.M. (1994). *Behaviour and Ecology of Grey-Cheeked Mangabeys* (Cercocebus albigena) *in the Lope Reserve*, *Gabon* [Doctoral dissertation, University of Stirling].

Harris, E. E. (2000). Molecular systematics of the Old World monkey tribe Papionini: Analysis of the total available genetic sequences. *Journal of Human Evolution*, *38*, 235–256.

Harris, E. E., & Disotell, T. R. (1998). Nuclear gene trees and the phylogenetic relationship of the mangabeys (primates: Papionini). *Molecular Biology and Evolution*, *15*, 892–900.

Hogg, R. T., & Walker, R. S. (2011). Life-history correlates of enamel microstructure in Cebidae (Platyrrhini, primates). *The Anatomical Record*, *294*(12), 2193–2206.

Jolly, C. J. (1970). The seed-eaters: A new model of hominid differentiation based on a baboon analogy. *Man*, *5*, 5–26.

Jolly, C. J. (2001). A proper study for mankind: Analogies from the Papionin monkeys and their implications for human evolution. *American Journal of Physical Anthropology*, *116*, 177–204.

Kay, R. F. (1978). Molar struture and diet in extant Cercopithecidae. In P. M. Butler & K. A. Joysey (Eds.), *Development, function and evolution of teeth* (pp. 309–340). Academic Press.

Kay, R. F. (1981). The nut-crackers - a new theory of the adaptations of the Ramapithecinae. *American Journal of Physical Anthropology*, *55*, 141–151.

Kim, A.C., (2019). *A comparison of molar morphology from extant Cercopithecid monkeys and Pliocene Parapapio from Makapansgat*, *South Africa using Elliptical Fourier Analysis* [Dissertation, Georgia State University].

Kitashima, F., Tomonari, H., Kuninori, T., Uehara, S., & Miyawaki, S. (2015). Modulation of the masticatory path at the mandibular first molar throughout the masticatory sequence of a hard gummy jelly in normal occlusion. *Cranio*, *33*(4), 263–271.

Komino, M., & Shiga, H. (2017). Changes in mandibular movement during chewing of different hardness foods. *Odontology*, *105*, 418–425.

Kono, R. T. (2004). Molar enamel thickness and distribution patterns in extant great apes and humans: New insights based on a 3-dimensional whole crown perspective. *Anthropological Science*, *112*, 121–146.

Kono, R. T., Suwa, G., & Tanijiri, T. (2002). A three dimensional analysis of enamel distribution patterns in human permanent first molars. *Archives Oral of Biology*, *47*, 867–875.

Kono-Takeuchi, R., Suwa, G., Kanazawa, E., & Tanijiri, T. (1998). A new method of evaluating enamel thickness based on a three-dimensional measuring system. *Anthropological Science*, *105*, 217–229.

Kupczik, K., & Lev-Tov Chattah, N. (2014). The adaptive significance of enamel loss in the mandibular incisors of cercopithecine primates (Mammalia: Cercopithecidae): A finite element modelling study. *PLoS One*, *9*(5), e97677.

Lambert, J.E., Chapman, C.A., Wrangham, R.W., &. N.L. Conklin-Brittain. (2004). Hardness of cercopithecine foods: Implications for the critical function of enamel thickness in exploiting fallback foods. *American Journal of Physical Anthropology*, *125*, 363–368.

Lawn, B. R., & Lee, J. J. (2009). Analysis of fracture and deformation modes in teeth subjected to occlusal loading. *Acta Biomaterialia*, *5*, 2213–2221.

Lawn, B. R., Lee, J. J. W., Constantino, P. L., & Lucas, P. W. (2009). Predicting failure in mammalian enamel. *Journal of the Mechanical Behavior of Biomedical Materials*, *2*, 33–42.

Lucas, P., Constantino, P., Wood, B., & Lawn, B. (2008). Dental enamel as a dietary indicator in mammals. *BioEssays*, *30*, 374–385.

Lucas, P. W., & Teaford, M. F. (1994). Functional morphology of colobine teeth. In A. G. Davies & J. F. Oates (Eds.), *Colobine Monkeys: Their Ecology*, *Behavior and Evolution* (pp. 173–204). Cambridge University Press.

Luke, D. A., & Lucas, P. W. (1983). The significance of cusps. *Journal of Oral Rehabilitation*, *10*, 197–206.

Macho, G. A., & Berner, M. E. (1994). Enamel thickness and the helicoidal occlusal plane. *American Journal of Physical Anthropology*, *94*, 327–337.

Macho, G. A., & Shimizu, D. (2009). Dietary adaptations of South African australopiths: Inference from enamel prism attitude. *Journal of Human Evolution*, *57*, 241–247.

Macho, G. A., & Thackeray, J. F. (1992). Computed tomography and enamel thickness of maxillary molars of Plio- Pleistocene hominids from Sterkfontein, Swartkrans, and Kromdraai (South Africa): An exploratory study. *American Journal of Physical Anthropology*, *89*, 133–143.

Macho, G. A., & Thackeray, J. F. (1993). Computed tomography and intercuspal angulation of maxillary molars of Plio-Pleistocene hominids from Sterkfontein, Swartkrans and Kromdraai (South Africa): An exploratory study. *Zeitschrift für Morphologie und Anthropologie*, *79*, 261–269.

Martin, L. (1985). Significance of enamel thickness in hominoid evolution. *Nature*, *314*, 260–263.

McGraw, W. S. (1994). Census, habitat preference and polyspecific associations of six monkeys in the Lomako Forest, Zaire. *American Journal of Primatology*, *34*, 295–307.

McGraw, W. S., & Daegling, D. J. (2020). Diet, feeding behavior, and jaw architecture of Taï monkeys: Congruence and chaos in the realm of functional morphology. *Evolutionary Anthropology: Issues, News, and Reviews*, *29*(1), 14–28.

McGraw, W. S., Pampush, J. D., & Daegling, D. J. (2012). Brief communication: Enamel thickness and durophagy in mangabeys revisited. *American Journal of Physical Anthropology*, *147*, 326–333.

McGraw, W. S., van Casteren, A., Kane, E., Geissler, E., & Daegling, D. J. (2016). Feeding and oral processing behaviors of two colobine monkeys in Taï Forest, Ivory Coast. *Journal of Human Evolution*, *98*, 90–102.

McGraw, W. S., Vick, A., & Daegling, D. J. (2011). Sex and age differences in the diet and ingestive behaviors of sooty mangabeys (*Cercocebus atys*) in the tai Forest, Ivory Coast. *American Journal of Physical Anthropology*, *144*, 140–153.

McGraw, W. S., Vick, A. E., & Daegling, D. J. (2014). Dietary variation and food hardness in sooty Mangabeys (*Cercocebus atys*): Implications for fallback foods and dental adaptation. *American Journal of Physical Anthropology*, *154*, 413–423.

Modesto-Mata, M., García-Campos, C., Martín-Francés, L., Martínez de Pinillos, M., García-Gonzalez, R., Quintino, Y., Canals, A., Lozano, M., Dean, M. C., Martinón-Torres, M., & Bermúdez de Castro, J. M. (2017). New methodology to reconstruct in 2-D the cuspal enamel of modern human lower molars. *American Journal of Physical Anthropology*, *163*, 824–834.

Molnar, S., & Gantt, D. G. (1977). Functional implications of primate enamel thickness. *American Journal of Physical Anthropology*, *46*, 447–454.

O'Hara, MC. 2021. *Features of catarrhine posterior dental crowns associated with durophagy: Implications for fossil hominins* [Doctoral dissertation, The Ohio State University].

O'Hara, M. C., & Guatelli-Steinberg, D. (2021). Reconstructing tooth crown heights and enamel caps: A comparative test of three existing methods with recommendations for their use. *The Anatomical Record*, *305*, 123–143. https://doi.org/10.1002/ar.24637

O'Hara, M. C., Le Cabec, A., Xing, S., Skinner, M. F., & Guatelli-Steinberg, D. (2019). Safe casting and reliable cusp reconstruction assisted by micro-computed tomographic scans of fossil teeth. *The Anatomical Record*, *302*, 1516–1535.

Olejniczak, A. J., & Grine, F. E. (2006). Assessment of the accuracy of dental enamel thickness measurements using microfocal X-ray computed tomography. *The Anatomical Record. Part A, Discoveries in Molecular, Cellular, and Evolutionary Biology*, *288*, 263–275.

Olejniczak, A. J., Martin, L. B., & Ulhaas, L. (2004). Quantification of dentine shape in anthropoid primates. *Annals of Anatomy-Anatomischer Anzeiger*, *186*, 479–485.

Olupot, W., Chapman, C. A., Waser, P. M., & Isabirye-Basuta, G. (1997). Mangabey (*Cercocebus albigena*) ranging patterns in relation to fruit availability and the risk of parasite infection in Kibale National Park, Uganda. *American Journal of Primatology*, *43*, 65–78.

Pampush, J. D., Duque, A. C., Burrows, B. R., Daegling, D. J., Kenney, D., W.F. & McGraw, W. S. (2013). Homoplasy and thick enamel in primates. *Journal of Human Evolution*, *64*, 216–224.

Poulsen, J. R., Clark, C. J., Connor, E. F., & Smith, T. B. (2002). Differential resource use by primates and hornbills: Implications for seed dispersal. *Ecology*, *83*, 228–240.

Poulsen, J. R., Clark, C. J., & Smith, T. B. (2001). Seasonal variation in the feeding ecology of the grey-cheeked mangabey (*Lophocebus albigena*) in Cameroon. *American Journal of Primatology*, *54*, 91–105.

Rabenold, D., & Pearson, O. M. (2011). Abrasive, silica phytoliths and the evolution of thick molar enamel in primates, with implications for the diet of *Paranthropus boisei*. *PLoS One*, *6*, e28379.

Rasmussen, D. T., Friscia, A. R., Gutierrez, M., Kappelman, J., Miller, E. R., Muteti, S., Reynoso, D., Rossie, J. B., Spell, T. L., Tabor, N. J., & Gierlowski-Kordesch, E. (2019). Primitive Old World monkey from the earliest Miocene of Kenya and the evolution of cercopithecoid bilophodonty. *Proceedings of the National Academy of Sciences*, *116*, 6051–6056.

Reid, D. J., Schwartz, G. T., Dean, M. C., & Chandrasekera, M. S. (1998). A histological reconstruction of dental development in the common chimpanzee, *pan troglodytes*. *Journal of Human Evolution*, *35*, 427–448.

SAS Institute Inc. (2015). *SAS/STAT® 14.1 User's Guide*. SAS Institute Inc.

Saunders, S. R., Chan, A. H., Kahlon, B., Kluge, H. F., & FitzGerald, C. M. (2007). Sexual dimorphism of the dental tissues in human permanent mandibular canines and third premolars. *American Journal of Physical Anthropology*, *133*, 735–740.

Schwartz, G. T. (1997). *Taxonomic & Functional Aspects of enamel cap structure in south African Plio-Pleistocene hominids: A high-resolution computed tomographic study*. *Department of Anthropology*. Washington University.

Schwartz, G. T. (2000). Taxonomic and functional aspects of the patterning of enamel thickness distribution in extant large-bodied hominoids. *American Journal of Physical Anthropology*, *111*, 221–244.

Schwartz, G. T., McGrosky, A., & Strait, D. S. (2020). Fracture mechanics, enamel thickness and the evolution of molar form in hominins. *Biology Letters*, *16*(1), 20190671.

Shimizu, D. (2002). Functional implications of enamel thickness in the lower molars of red colobus (Procolobus badius) and Japanese macaque (*Macaca fuscata*). *Journal of Human Evolution*, *43*, 605–620.

Skinner, M. M., Alemseged, Z., Gaunitz, C., & Hublin, J. J. (2015). Enamel thickness trends in Plio- Pleistocene hominin mandibular molars. *Journal of Human Evolution*, *85*, 35–45.

Smith, T. M., Bacon, A.-M., Demeter, F., Kullmer, O., Nguyen, K. T., de Vos, J., Wang, W., Zermeno, J., & Zhang, L. (2011). Dental tissue proportions in fossil orangutans from mainland Asia and Indonesia. *Human Origins Research*, *1*, 1–6.

Smith, T. M., Kupczik, K., Machanda, Z., Skinner, M. M., & Zermeno, J. P. (2012). Enamel thickness in Bornean and Sumatran orangutan dentitions. *American Journal of Physical Anthropology*, *147*, 417–426.

Spoor, C. F., Zonneveld, F. W., & Macho, G. A. (1993). Linear measurements of cortical bone and dental enamel by computed tomography: Applications and problems. *American Journal of Physical Anthropology*, *91*, 469–484.

Strait, D. S., Constantino, P., Lucas, P. W., Richmond, R. G., Spencer, M. A., Dechow, P. C., Ross, C. F., Grosse, I. R., Wright, B. W., Wood, B. A., Weber, G. W., Wang, Q., Byron, C., Slice, D. E., Chalk, J., Smith, A. L., Smith, L. C., Wood, S., Berthaume, M., … Ledogar, J. A. (2013). Viewpoints: Diet and dietary adaptations in early hominins: The hard food perspective. *American Journal of Physical Anthropology*, *151*, 339–355.

Strasser, E., & Delson, E. (1987). Cladistic analysis of cercopithecid relationships. *Journal of Human Evolution*, *16*(1), 81–99.

Suwa, G., & Kono, R. T. (2005). A micro-CT based study of linear enamel thickness in the mesial cusp section of human molars: Reevaluation of methodology and assessment of within-tooth, serial, and individual variation. *Anthropological Science*, *113*, 273–289.

Thiery, G., Lazzari, V., Ramdarshan, A., & Guy, F. (2017). Beyond the map: Enamel distribution characterized from 3D dental topography. *Frontiers in Physiology*, *8*, 524.

Tutin, C. E., Ham, R. M., White, L. J., & Harrison, M. J. (1997). The primate community of the Lopé reserve, Gabon: Diets, responses to fruit scarcity, and effects on biomass. *American Journal of Primatology*, *42*, 1–24.

Ulhaas, L., Henke, W., & Rothe, H. (1999). Variation in molar enamel thickness of the genera *Cercopithecus* and *colobus*. *L'Anthropologie*, *37*, 265–271.

van Casteren, A., Wright, E., Kupczik, K., & Robbins, M. M. (2019). Unexpected hard-object feeding in Western lowland gorillas. *American Journal of Physical Anthropology*, *170*, 433–438.

Vogel, E. R., van Woerden, J. T., Lucas, P. W., Utami Atmoko, S. S., van Schaik, C. P., & Dominy, N. J. (2008). Functional ecology and evolution

of hominoid molar enamel thickness: *Pan troglodytes schweinfurthii* and *Pongo pygmaeus wurmbii*. *Journal of Human Evolution*, *55*, 60–74.

Waser, P. M. (1984). Ecological differences and behavioral contrasts between two mangabey species. In P. S. Rodman & J. G. H. Cant (Eds.), *Adaptations for Foraging in Nonhuman Primates* (pp. 195–216). Columbia University Press.

Woda, A., Foster, K., Mishellany, A., & Peyron, M. A. (2006). Adaptation of healthy mastication to factor pertaining to the individual or to the food. *Physiology & Behavior*, *89*, 28–35.

How to cite this article: Guatelli-Steinberg, D., Schwartz, G. T., O'Hara, M. C., Gurian, K., Rychel, J., & McGraw, W. S. (2022). Molar form, enamel growth, and durophagy in *Cercocebus* and *Lophocebus*. *American Journal of Biological Anthropology*, 1–19. https://doi.org/10.1002/ajpa.24592